

C–D₀ (D₀ = π -donor, F) Cleavage in H₂C=CH(D₀) by (Cp₂ZrHCl)_n: Mechanism, Agostic Fluorines, and a Carbene of Zr(IV)

Lori A. Watson, Dmitry V. Yandulov, and Kenneth G. Caulton*

Contribution from the Department of Chemistry, Indiana University, Bloomington, Indiana 47405-7102

Received July 5, 2000

Abstract: Consistent with the C–O cleavage behavior of vinyl ethers, vinyl fluoride reacts with Cp₂ZrHCl to give Cp₂ZrFCl and C₂H₄ as primary products. DFT (B3PW91) calculations show this reaction to be highly exoenergetic (–55 kcal/mol), and reveal a σ -bond metathesis mechanism to be unfavorable compared to a Zr–H addition across the C=C bond, with regiochemistry placing F on C _{β} of the resulting fluoroethyl ligand. β -F elimination (onto Zr) then completes the reaction. There is no η^2 -olefin intermediate on the reaction path. DFT calculations seeking the energy and structure of the two carbenes Cp₂ZrHCl[CF(CH₃)] and Cp₂ZrFCl[CH(CH₃)] are also described.

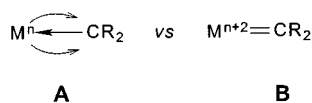
Introduction

The molecular fragment RuHClL₂ (L = PⁱPr₃), derived from the dimer [RuH(μ -Cl)L₂]₂, has proven¹ to be a π -rich species which readily and selectively converts olefins containing π -donor substituents (D₀) into carbene ligands (eq 1). The



exothermic character of *this* transformation (an unusually easy route to a carbene, and one which is 40–70 kcal/mol endothermic for forming the *free* carbene) relies on π -electron donation to the carbene carbon by both D₀ and by the metal. Taube showed² long ago that the d⁶ configuration for Ru and Os is very reducing, which is equivalent to π -donating (back-donating).

Exploring the analogous chemistry for a d⁰ metal offers the possibility of very different thermodynamic preferences. For example, nonheteroatom stabilized carbenes (the so-called Schrock carbenes) must rely wholly on metal back-donation to occupy the carbene p orbital. This is why such carbenes generally involve highly electropositive metals in low formal oxidation states (considering the carbene as uncharged). Note also that the neutral carbene formalism with much back-bonding (A) is not different from the dianionic carbene formalism (B).



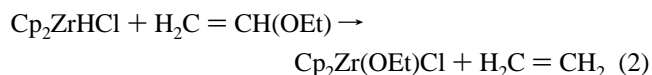
The present work is thus directed in part at exploring both experimentally and computationally the accessibility to a carbene ligand in an unprecedented environment: one with no d electrons to contribute to the carbene (C). In fact, there are no



known molecules where a neutral carbene is bound to a d⁰ metal.³ This makes a species such as Cp₂ZrHCl[CF(CH₃)] or Cp₂ZrFCl[CH(CH₃)] attractive from the structural point of view. What is the bond order of the Zr/carbene bond and how will the carbene p orbital acquire electron density? To put this into perspective, a few d⁰ carbonyl complexes *are* known,⁴ for example, Cp₂Ti(CO)₂²⁺ and Cp₂Zr(acetyl)(CO)⁺, and the bonding in Cp*₂Zr(H)₂(CO) has been discussed^{4i,j} with regard to its surprisingly low ν_{CO} value.

Zirconium is termed “oxo-philic”, and is, more generally, considered to form strong bonds with any light atom which bears multiple lone pairs: amides, halides, and pseudohalides. It is for this reason that olefins bearing such π -donor functionality cannot be successfully polymerized by zirconium olefin polymerization catalysts: the functionality is abstracted from carbon, thereby poisoning the catalyst.

The early stoichiometric applications of Schwartz’ reagent, Cp₂ZrHCl, are consistent with the above principle: they generally involved nonfunctionalized olefins and alkynes.⁵ Subsequent studies⁶ of Cp₂ZrHCl reacting with vinyl ethers H₂C=CH(OR) confirmed the ability of this Lewis acidic zirconium to “abstract” an OR group by C/O bond cleavage (eq 2)



The released olefin was then rapidly hydrozirconated by additional Cp₂ZrHCl to give Cp₂Zr(C₂H₅)Cl.

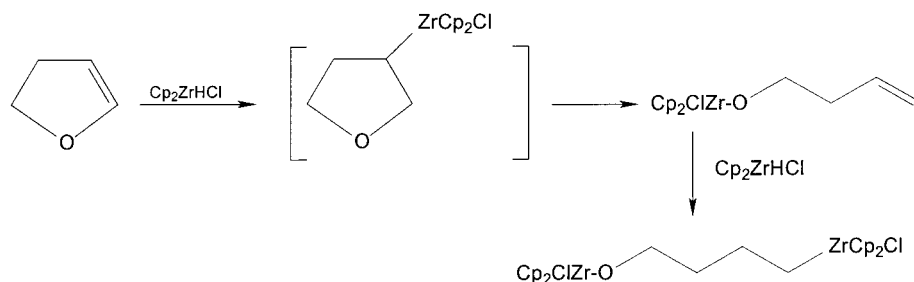
While examples of early transition metal complexes which cleave the strong C–F bond⁷ are not as plentiful as those of

(1) (a) Coalter, J. N., III; Spivak, G. J.; Gérard, H.; Clot, E.; Davidson, E. R.; Eisenstein, O.; Caulton, K. G. *J. Am. Chem. Soc.* **1998**, *120*, 9388. (b) Coalter, J. N., III; Bollinger, J. C.; Huffman, J. C.; Werner-Zwanziger, U.; Caulton, K. G.; Davidson, E. R.; Gérard, H.; Clot, E.; Eisenstein, O. *New J. Chem.* **2000**, *24*, 9.

(2) Taube, H. *Pure Appl. Chem.* **1979**, *51*, 901.

(3) A reviewer has commented that Arduengo carbenes are known to coordinate to d⁰ metal centers. Since such carbenes involve much N \rightarrow C donation from the two heteroatoms on the carbene carbon, this behavior towards d⁰ metals is predictable. Indeed, Arduengo carbenes are now proven to be primarily σ -donors, not π -acceptors towards metals: Herrmann, W. A.; Kocher, C. *Angew. Chem., Int. Ed.* **1998**, *37*, 2490.

Scheme 1



latter metals,⁸ there has been a recent report of $[\text{Cp}_2\text{ZrH}_2]_2$ reacting with C_6F_6 to give $\text{Cp}_2\text{Zr}(\text{C}_6\text{F}_5)\text{F}$ as the major product.⁹

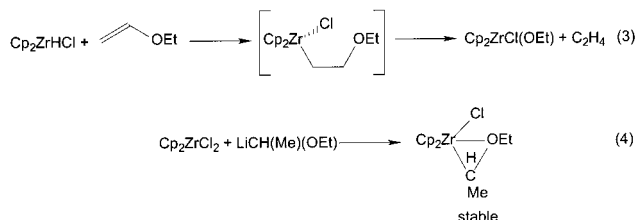
In contrast, reaction of Schwartz's reagent with vinyl phosphines forms a nonagostic insertion product, which undergoes no further reaction.¹⁰ Thus, the qualitative trend of zirconium interacting much more strongly with first row "hard" bases and rejecting other "softer" heteroatoms is again demonstrated.

Our interest here is in the mechanism of such C/heteroatom cleavage by Zr(IV). The absence of d electrons makes this an electrophilic, not an oxidative process, and indeed, it is for the Cp_2ZrXY unit that the σ -bond metathesis mechanism was devised out of a necessity to avoid the more traditional oxidative mechanisms.¹¹ Our special focus here will be on C–F bond scission, since this is a thermodynamically quite strong bond, and one subject to intense recent study.^{12,8a} The specific organofluorine target is vinyl fluoride.

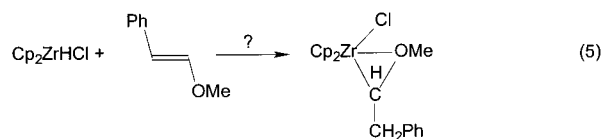
Results

Vinyl Ethers. The reaction of Cp_2ZrHCl with ethyl vinyl ether has been reported⁶ to yield $\text{Cp}_2\text{ZrCl}(\text{OEt})$ and ethylene as primary products. This was shown to proceed by the regiochemistry of eq 3 because independent synthesis of the opposite

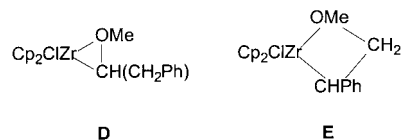
regioisomer (eq 4) showed it to be stable (i.e., no C/O bond scission) under the conditions of eq 3.



We chose β -methoxy styrene as a vinyl ether in which steric effects at the α -carbon might be anticipated to direct the regiochemistry away from that of ethyl vinyl ether. This attempt (eq 5) apparently fails since the products of this reaction



(complete in C_6D_6 within 1.5 h at 25 °C) are $\text{Cp}_2\text{ZrCl}(\text{OMe})$ and the result of secondary reaction of liberated styrene with Cp_2ZrHCl : $\text{Cp}_2\text{ZrCl}(\text{CH}_2\text{CH}_2\text{Ph})$ and $\text{Cp}_2(\text{Cl})\text{ZrCHPhCH}_3$ (minor product). The former has equivalent Cp rings and an AA'XX' spin system pattern for the $-\text{CH}_2\text{CH}_2-$ group. The $^1\text{H}/^1\text{H}$ coupling within this spin system was confirmed by a COSY study, and the presence of two CH_2 groups (contrast **D** and **E**, which have only one CH_2 group) was established by



HMQC and DEPT experiments. This same product was also synthesized independently from styrene and Cp_2ZrHCl . If the reaction is executed in the stoichiometry $1\text{Cp}_2\text{ZrHCl}:2(\text{Ph})\text{-HC}=\text{CH}(\text{OMe})$, free styrene is in fact observed.

Similar results are obtained (Scheme 1) with cyclic vinyl ethers (2,3-dihydrofuran or 3,4-dihydro-2H-pyran, for example).¹³ Once again, the olefin inserts into the Zr–H bond through an initial Zr–O agostic interaction, and then was suggested to undergo C–O bond cleavage to form the alkoxides. This affords the acyclic species $\text{Cp}_2\text{Zr}(\text{Cl})\text{O}(\text{CH}_2)_x\text{CH}=\text{CH}_2$ which can further react with a second equivalent of Cp_2ZrHCl to form a dizirconated species.

C/O bond cleavage is the shared feature of these reactions, but it must not be interpreted as indicating the complete absence

(4) (a) Meyer, T. J. *J. Am. Chem. Soc.* **1976**, *98*, 6733. (b) Manriquez, J. M.; McAlister, D. R.; Sanner, R. D.; Bercaw, J. E. *J. Am. Chem. Soc.* **1978**, *100*, 2716. (c) Antonelli, D. M.; Tjaden, E. B.; Stryker, J. M. *Organometallics* **1994**, *13*, 763. (d) Guo, Z.; Swenson, D. C.; Guram, A. S.; Jordan, R. F. *Organometallics* **1994**, *13*, 766. (e) Howard, W. A.; Parkin, G.; Rheingold, A. *Polyhedron* **1995**, *14*, 25. (f) Procopio, L. J.; Carroll, P. J.; Berry, D. H. *Polyhedron* **1995**, *14*, 45. (g) Calderazzo, F.; Pampaloni, G.; Tripepi, G. *Organometallics* **1997**, *16*, 4943. (h) Pampaloni, G.; Tripepi, G. *J. Organomet. Chem.* **2000**, *593*, 20. (i) Brintzinger, H. H. *J. Organomet. Chem.* **1979**, *171*, 337. (j) Marsella, J. A.; Curtis, C. J.; Bercaw, J. E.; Caulton, K. G. *J. Am. Chem. Soc.* **1980**, *102*, 7244.

(5) (a) Hart, D. W.; Schwartz, J. *J. Am. Chem. Soc.* **1974**, *96*, 8115. (b) Labinger, J. A.; Hart, D. W.; Seibert, W. E., III; Schwartz, J. *J. Am. Chem. Soc.* **1975**, *97*, 3851. (c) Hart, D. W.; Blackburn, T. F.; Schwartz, J. *J. Am. Chem. Soc.* **1975**, *97*, 679. (d) Schwartz, J.; Labinger, J. A. *Angew. Chem., Int. Ed. Engl.* **1976**, *15*, 333. (e) Wipf, P.; John, H. *Tetrahedron* **1996**, *52*, 1253.

(6) Buchwald, S. L.; Nielson, R. B.; Dewan, J. C. *Organometallics* **1988**, *7*, 2324.

(7) (a) Burns, C. J.; Anderson, R. A. *J. Chem. Soc., Chem. Commun.* **1989**, 136. (b) Watson, P. L.; Tulip, T. H.; Williams, I. *Organometallics* **1990**, *9*, 1999. (c) Weydert, M.; Anderson, R. A.; Bergman, R. G. *J. Chem. Soc.* **1993**, *115*, 8837.

(8) (a) Kiplinger, J. L.; Richmond, T. G.; Osterburg, C. E. *Chem. Rev.* **1994**, *94*, 373. (b) Murphy, E. F.; Murugavel, R.; Roesky, H. W. *Chem. Rev.* **1997**, *97*, 3425.

(9) Edelbach, B. L.; Rahman, A. K. F.; Lachicotte, R. J.; Jones, W. D. *Organometallics* **1999**, *18*, 3170.

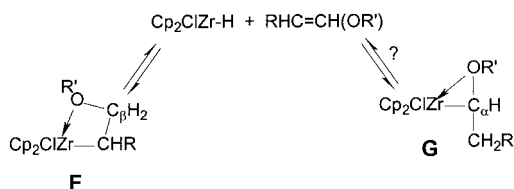
(10) Zablocka, M.; Igau, A.; Majoral, J.-P.; Pietrusiewicz, K. M. *Organometallics* **1993**, *12*, 603.

(11) (a) Koga, N.; Morokuma, K. *Chem. Rev.* **1991**, *91*, 823. (b) Tolbert, M. A.; Beauchamp, J. L. *J. Am. Chem. Soc.* **1984**, *106*, 8117. (c) Thompson, M. E.; Baxter, S. M.; Bulls, A. R.; Burger, B. J.; Nolan, M. C.; Santarsiero, B. D.; Schaefer, W. P.; Bercaw, J. E. *J. Am. Chem. Soc.* **1987**, *109*, 203. (d) Christ, C. S.; Eyster, J. R.; Richardson, D. E. *J. Am. Chem. Soc.* **1990**, *112*, 596.

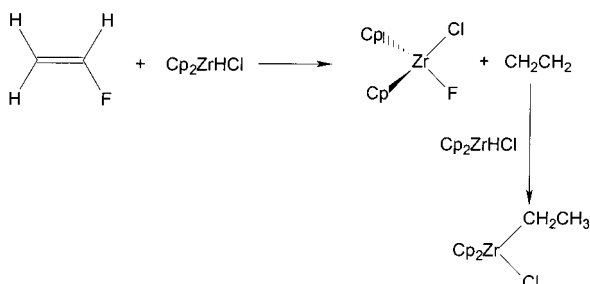
(12) Burdeniuc, J.; Jedlicka, B.; Crabtree, R. H. *Chem. Ber. Recl.* **1997**, *97*, 3425.

(13) Cénac, N.; Zablocka, M.; Igau, A.; Commenyes, G.; Majoral, J. P.; Skowronska, A. *Organometallics* **1996**, *15*, 1208.

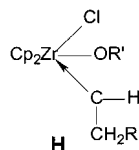
Scheme 2



Scheme 3



of Zr–H addition with the opposite regiochemistry (Scheme 2) since that *might* be reversible. For the later transition metal Rh^{III}, and where O → metal donation is not possible, it is thermodynamically favored to have OR' on C_α rather than (C_β).¹⁴ Such thermodynamic preference could certainly be reversed when an O → metal bond is involved, and where ring sizes differ. In the cases at hand, formation of the ultimately preferred Zr–alkoxide linkage can only evolve from F, since G has put the hydrogen on the “wrong” carbon for an olefinic product. Indeed, from G, what might evolve is the carbene species H.



Vinyl Fluoride. A slurry of Cp₂ZrHCl in benzene reacts to completion within 1.5 h with vinyl fluoride (100% excess). Cp₂Zr(C₂H₅)Cl, which is the product of the secondary reaction of Cp₂ZrHCl with liberated ethylene is evident by Cp and ethyl ¹H NMR signals. The continued production of this compound diminishes with time, and free ethylene accumulates, due to the depletion of Cp₂ZrHCl. Three additional Cp resonances and two ¹⁹F resonances grow during the reaction. Two of these show somewhat broader Cp ¹H NMR resonances, consistent with unresolved coupling to ¹⁹F. These three Cp and two ¹⁹F resonances are attributed to Cp₂ZrClF and the F/Cl redistribution products Cp₂ZrCl₂, Cp₂ZrF₂ and Cp₂Zr(C₂H₅)F. Overall, these results are explained by the reaction in Scheme 3.

Attempts to independently synthesize Cp₂ZrF₂ have been successful. As Cp₂ZrF₂ is soluble in THF, it was hoped that comparison of its chemical shift with the chemical shifts of the products of the reaction of vinyl fluoride and Cp₂ZrHCl in THF-*d*₈ could provide a basis for assigning at least the Cp resonance of the supposed difluoride halide exchange product. In this reaction in THF-*d*₈, the analogous products were obtained, with Cp₂ZrCl(CH₂CH₃) and free ethylene both observed. One of the Cp resonances at 6.37 matches well in shift and line width with the Cp signal of Cp₂ZrF₂ at 6.38 ppm. The ¹⁹F shift of the difluoride at –157.3 is not seen as a distinct peak in the ¹⁹F of

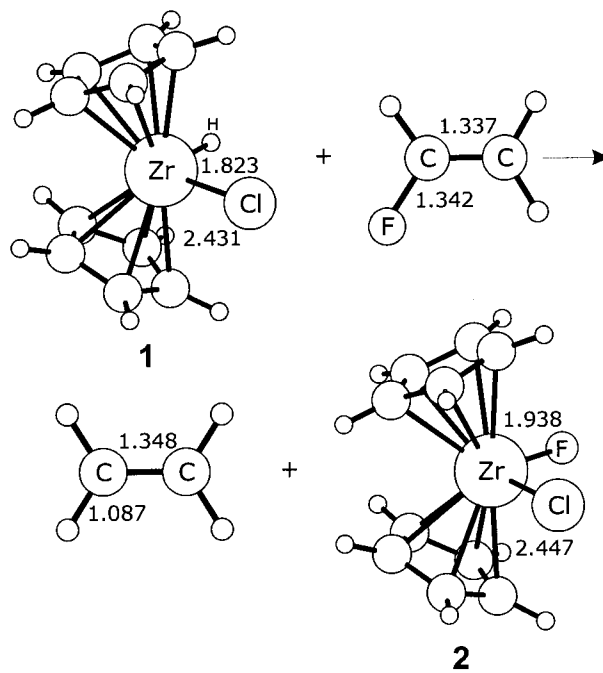


Figure 1. Optimized geometries of reactants and products with selected distances in Å.

the product mixture; however, a broad resonance at approximately the same chemical shift is observed. This resonance might be broadened because of halide exchange with other products in the reaction mixture.

No intermediates were observed in the course of this reaction. In particular, no fluoroethyl complex or carbene species was observed. The approximately 1.5-h reaction time is mass-transfer limited, due to the extremely low solubility of Cp₂ZrHCl. Thus, kinetic studies will not depend on the molecular mechanism of this reaction. We therefore undertook DFT calculations to delineate the reaction mechanism (see below).

To generalize this reactivity of fluorine-substituted olefins, CH₂CF₂ was reacted with Cp₂ZrHCl; this reaction produces CH₂CHF, Cp₂Zr(CH₂CH₃)Cl, and CH₂CH₂ (¹H NMR evidence). Again, the products formed indicate that the primary reaction gives Cp₂ZrClF and, in this case, vinyl fluoride, which can then react with another equivalent of Cp₂ZrHCl.

Calculated Reaction Energy. DFT calculations were carried out on the overall reaction (Figure 1). Species 1 and 2 are very similar in their arrangement of Cp ligands, differing significantly only in the Zr–Cl bond distance. The Zr–Cl bond lengthens by 0.016 Å from the reactant, Cp₂ZrHCl, to the product, Cp₂ZrClF. This is probably due to the increased donor ability of F versus H, allowing slight lengthening of the Zr–Cl bond. The Cp (centroid)–Zr–Cp–(centroid) angle changes very little throughout the reaction; the average of all calculated structures reported in this study is 131.6°, with a standard deviation of 1.65°.

The overall reaction energy (with zero-point energy correction included) was calculated to be –55.1 kcal/mol. This large exothermic value is to be expected considering the strength of the Zr–F bond formed.^{15,16}

Mechanistic Questions. Because no intermediates were observed for this reaction, DFT methods were used to evaluate a number of mechanistic questions. DFT calculations on the analogous reaction with C₂H₄ have been published.¹⁷ One can

(14) Mak, K. W.; Xue, F.; Mak, T. C. W.; Chan, K. S. *J. Chem. Soc., Dalton Trans.* **1999**, 3333.

(15) Dias, A. R.; Martinho-Simoes, J. A. *Polyhedron* **1988**, *7*, 1531.

(16) Wipf, P.; Jahn, H. *Tetrahedron* **1996**, *52*, 12853.

(17) Endo, J.; Koga, N.; Morokuma, K. *Organometallics* **1993**, *12*, 2777.

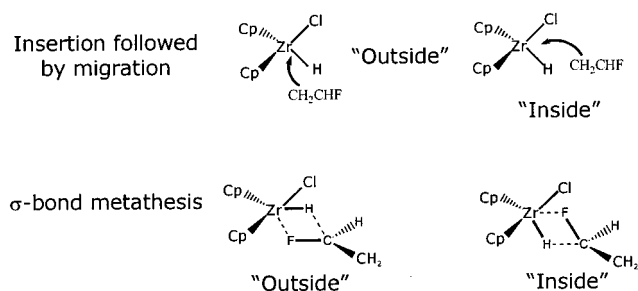


Figure 2. Possible mechanisms and approach directions.

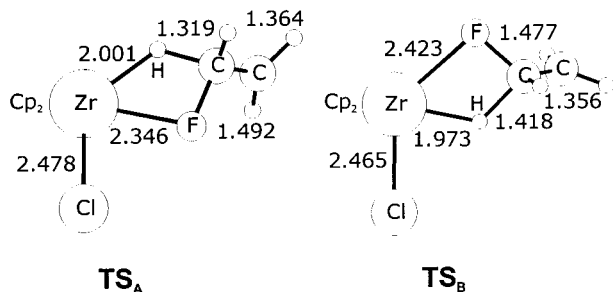


Figure 3. σ -Bond metathesis transition states: “inside” (TS_A) and “outside” (TS_B) with selected distances in Å.

imagine two classes of mechanisms that would lead to the observed experimental products (Figure 2). The olefin could first insert into the Zr–H bond and then undergo β -F migration and ethylene elimination. This mechanism corresponds to the olefin entering with the π_{cc} face first. Alternately, a four-centered transition state corresponding to a σ -bond metathesis mechanism could be formed. This would be the result of the F–C bond encountering the zirconium center first. Both of these mechanisms have been implicated in the reactions of early transition metals, and both are allowed by the unsaturated metal center in this case.

In each of these mechanisms, the olefin can approach from two directions, between the hydride and chloride (“inside”) or on the side opposite the chloride (“outside”); the third direction, approach opposite hydride, will not lead to the needed hydride–olefin interaction. There are also two possible regiochemistries of addition; the first of these forms an initial β -fluoro alkyl product, while insertion from the opposite direction will form an ethyl product with the fluorine on the α -carbon. Although only the β -fluoro interaction can lead to the observed products, the energetic difference between the two addition regiochemistries leads to interesting conclusions and therefore will be discussed later.

σ -Bond Metathesis. As zirconium(IV) has vacant d orbitals available, a four-centered transition state is possible. Indeed, σ -bond metathesis was first proposed to account for these same types of reactions with d^0 metals—particularly zirconium.¹¹ Additionally, such a concerted transition state has been proposed as the mechanism in the C–F bond cleavage of a variety of fluoroarenes by a similar system, $[\text{Cp}_2\text{ZrH}_2]_2$.⁹

A transition state was found for the “inside” approach of $\text{CH}_2\text{-CHF}$, forming a four-centered transition state TS_A (Figure 3). This structure can best be described as one resulting from electrophile-assisted nucleophilic attack. This is supported by the obvious pyramidalization of the α -carbon (sum of angles around the carbon is 343.5°) by the incoming hydride ligand and the weakening of the C–F bond as it interacts with Zr. In this transition state, the developing C–H bond is not very far advanced, as is evident by a C–H bond distance of 1.319 Å (compared to the C–H distance of 1.087 Å in free ethylene).

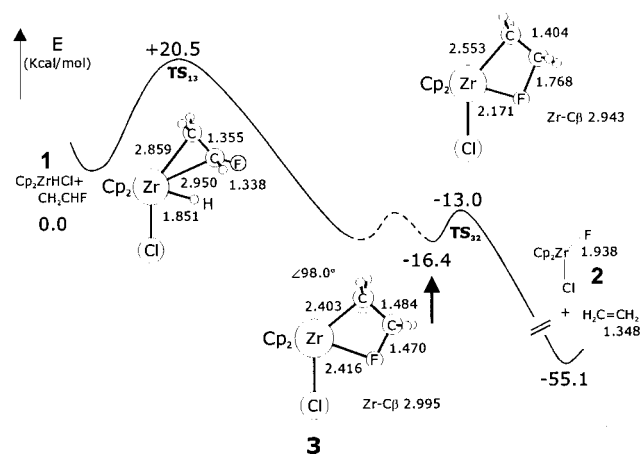
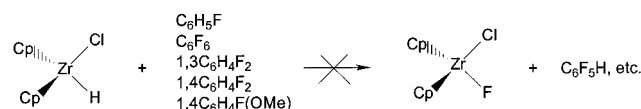


Figure 4. “Outside” reaction pathway, with selected bond distances (Å), angles (deg), and relative energies (with ZPE) in kcal/mol.

Scheme 4



The C–F bond is also stretched by 0.150 Å from its vinyl fluoride length as it begins to interact with zirconium. There is very little disruption of the C–C bond, however. It remains essentially a double bond, stretched by only 0.016 Å from the CH_2CHF distance of 1.348 Å.

The energy of this transition state lies 21.1 kcal/mol above the separated species. Using a typical¹⁸ ΔS^\ddagger of $-27 \text{ cal deg}^{-1} \text{ mol}^{-1}$, this corresponds to a half-life (when $[\text{C}_2\text{H}_3\text{F}] = 1 \text{ M}$) of $8 \times 10^4 \text{ h}$ at 25 °C. In reality, other pathways have a lower energy barrier.

A similar geometry, but with a higher activation energy, is obtained as a four-centered transition state from the “outside” approach (TS_B). The energy of this transition state lies 28.2 kcal/mol above the separated species and lies earlier still on the reaction coordinate than the “inside” case. Bonds being formed are further away from their product value. For example, the Zr–F bond is longer (at 2.423 Å) than in the “inside” transition state (2.346 Å) as is the developing C–H bond (1.418 vs 1.319 Å) (Figure 3).

Regardless of olefin approach trajectory, the experimental evidence in this case argues against the σ -bond metathesis mechanism. Namely, we did not observe C–F activation when Cp_2ZrHCl was reacted with a variety of fluoroarenes in a variety of concentrations (Scheme 4, 1.5 equiv, or neat arene). If σ -bond metathesis had been the operative mechanism, one would have expected the formation of Cp_2ZrClF and the corresponding arene. However, one would expect no reaction with the arenes if insertion was the predominant mechanism because insertion is more difficult with aromatic systems than for an isolated vinyl group due to loss of aromaticity. Thus, the fact that no reaction with arene was seen even with extended reaction time (3 days at room temperature) argues against a σ -bond metathesis mechanism and for one that allows an initial insertion step.

Insertion Mechanisms. (a) “Outside” Attack. Attack of the olefin *face* from the side opposite chloride is calculated to encounter a +20.5 kcal/mol barrier to insertion (Figure 4). The Zr–C distances (2.859 and 2.950 Å) at the TS_{13} indicate that relatively little Zr/olefin bond formation has taken place. For

(18) Minas da Piedade, M. E.; Simões, J. A. M. *J. Organomet. Chem.* **1996**, *518*, 167.

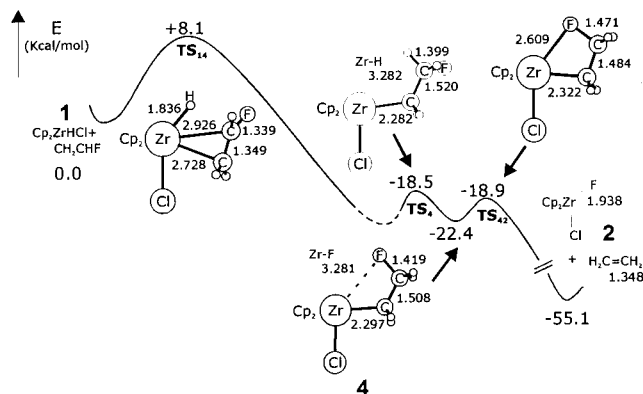


Figure 5. “Inside” reaction pathway, with selected bond distances (Å), angles (deg), and relative energies (with ZPE) in kcal/mol.

comparison, Zr(IV)/C(olefin) distances of 2.68 and 2.89 Å have been reported.¹⁹ There is no η^2 intermediate found here; the only η^2 -structure is this transition state. This is not surprising, as Zr in this instance has no d-electrons to stabilize an olefin complex by back-bonding. The high barrier is in contrast to the low barrier one would expect for a normal Lewis acid/base adduct (about 3 kcal/mol). While the higher calculated barrier is partly due to the lack of such an η^2 -intermediate, the hydride and chloride must move much closer together (from 100.2° in Cp₂ZrHCl to 74.0° in the transition state), providing some destabilization from H/Cl repulsive forces.

From the initial insertion transition state, a β -H agostic structure should be formed. While no *minimum* (i.e., intermediate) with this structure has been found, a product resulting from rotation about the CH₂F group, the β -F agostic structure (**3**), is a minimum. This lies 16.4 kcal/mol below the reactants, and shows lengthening of the C–F bond and a close F–Zr contact characteristic of an agostic structure.²⁰ Additionally, the agostic character is evident by a reduction in the Zr–C _{α} –C _{β} angle to 98.0°. A C–C distance of 1.484 Å, much nearer a C–C single bond length, implies that this structure is best described as a β -F agostic ethyl complex. Supporting this is the Zr–C _{β} bond distance, which at 2.995 Å is not within normal bonding distance (2.2–2.4 Å).

From this minimum, a transition state (TS₃₂) is formed which connects (**3**) to the final products. This transition state is surprisingly low in energy, lying only about 3.4 kcal/mol above the agostic intermediate.

Geometric parameters change in the expected manner throughout the reaction coordinate. The C–C bond, which begins as 1.348 Å in CH₂CHF lengthens to 1.355 Å at TS₁₃. It lengthens further to 1.484 Å at **3**, consistent with the formation of an alkyl fragment, before shortening to 1.404 Å in TS₃₂, in preparation for the elimination of ethylene. A similar trend is seen in the continuous stretching of the C–F distance from 1.338 in TS₁₃ to 1.470 in **3** and finally 1.768 Å in TS₃₂. The Zr–F bond shortens correspondingly from 2.416 in **3** to 1.938 Å in the final Cp₂ZrClF product (**2**).

(b) “Inside” Attack. Attack of the olefin between the hydride and chloride ligands provides a much lower activation barrier of +8.1 kcal/mol (Figure 5). This lower barrier to insertion might be explained by less steric repulsion from the cyclopentadienyl ligands when the olefin is in this “inside” position

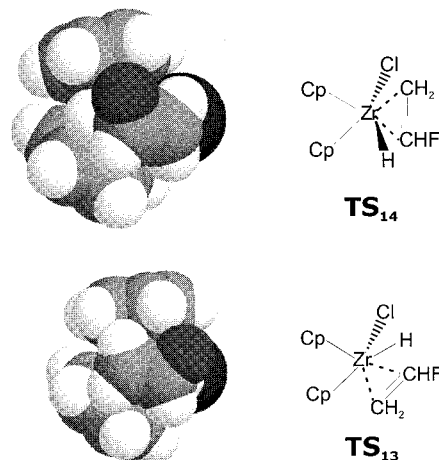


Figure 6. Space filling drawings of TS₁₃ and TS₁₄. Cl and F are darkest.

(Figure 6). The olefin, instead of being sandwiched between the two Cp rings as in the “outside” case, occupies a less sterically crowded face of the zirconium where there is more room between the Cp’s. Also, the Cl–Zr–H angle opens up to 140°, which eliminates any repulsion between the hydride and chloride ligands that may have been present in the “outside” case. Once again, there is no intermediate η^2 olefin complex (optimization of TS₁₄ distorted toward the reactants resulted in complete dissociation of H₂C=CHF); an η^2 adduct is a transition state for insertion.

The next step on the calculated reaction pathway is a transition state corresponding to CH₂F rotation to form a β -fluoroethyl intermediate (TS₄). This transition state has an energy of –18.5 kcal/mol below reactants. The β -hydrogen is nearly coplanar with Zr, C _{α} , and C _{β} ; the dihedral angle is 353.9°. The C–C bond distance indicates that this structure is very similar to an η^1 alkyl; the in-plane hydrogen appears not to interact strongly with the Zr center (C _{β} –H distance of 1.099 vs 1.098 for the noncoplanar hydrogen).

In contrast to the β -fluoro agostic structure seen in the “outside” reaction pathway (**3**), the β -fluoroethyl intermediate in the “inside” path, **4**, has an essentially nonbonding Zr–F distance (3.281 Å); minor stretching of the C–F bond is seen (1.399 in TS₄, vs 1.419 Å in **4**). The values, both taken from sp³ carbons, can also be compared with a different conformation where the CH₂F group has no interaction at all with the metal center, **5**, (Figure 7); in this case, the weakly agostic β -fluoroethyl C–F bond is still stretched (1.419 vs 1.401 Å for the noninteracting case).

As in the “outside” path, the energy rise from **4** to TS₄₂ is very small: 3.5 kcal/mol. The Zr–C _{β} distance is only slightly longer in this “inside” transition state than in TS₃₂ of the “outside” path, at 3.034 vs 2.943 Å, respectively.

The geometric parameters again correlate with the expected changes in structure along the reaction coordinate. For example, the C–C bond distance goes from a double bond distance of 1.349 in TS₁₄ to an η^1 -alkyl like 1.508 in **4**. This bond then shortens to 1.484 Å in TS₄₂ in preparation for the elimination of ethylene (C=C distance of 1.348 Å). The C–F bond lengthens throughout the reaction path, going from 1.339 to 1.399 to 1.419 to 1.471 Å for TS₁₄, TS₄, **4**, and TS₄₂. The Zr–F distance is also correspondingly shorter, decreasing dramatically from 3.281 Å in **4** to 2.609 Å in TS₄₂ in preparation for its final value of 1.938 Å in **2**. One other parameter which is interesting to follow is the Zr–C _{α} distance. It shortens considerably from TS₁₄ to **4** (2.728 to 2.297 Å), which is expected as a

(19) Wu, Z.; Jordan, R. F.; Petersen, J. L. *J. Am. Chem. Soc.* **1995**, *117*, 5867; Carpentier, J.-F.; Wu, Z.; Lee, C. W.; Strömberg, S.; Christopher, J. N.; Jordan, R. F. *J. Am. Chem. Soc.* **2000**, *122*, 7750.

(20) In agreement with literature precedent, we will refer to this as an agostic interaction. See Brothers, P. J.; Roper, W. R. *Chem. Rev.* **1988**, *88*, 1293.

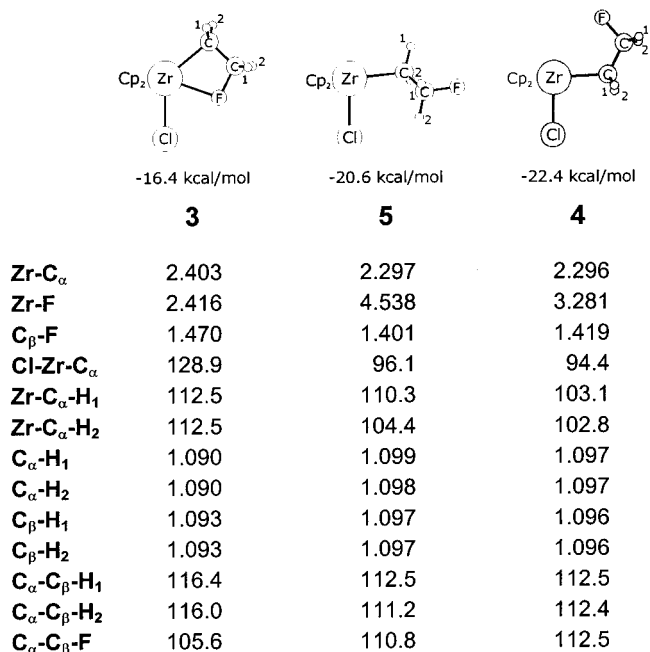


Figure 7. Selected bond distances (in Å), angles (in degrees) of β -fluoroethyl intermediates.

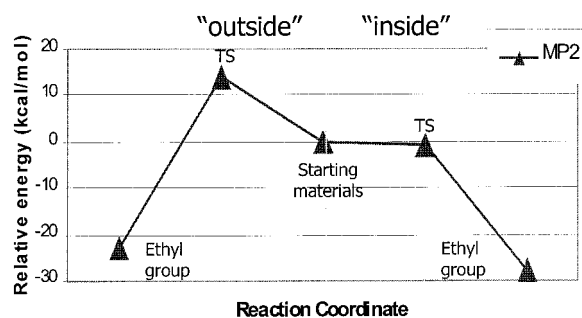


Figure 8. Energetics of hydrozirconation of CH_2CH_2 .¹⁷

structure similar to a simple η^1 alkyl is formed. This distance then lengthens again (to 2.322 Å in TS_{42}) in preparation for the elimination of ethylene.

General Conclusions about the Insertion Pathways. In both the inside and outside insertion pathways, no π -olefin complex exists as an intermediate at the chosen level of theory. Instead, the only π -olefin complexes found corresponded to transition states. A preference for the inside LUMO is seen in the difference between the energies of both the initial insertion transition states as well as in the β -fluoroethyl structures (see below). From the small energy cost to go from the fluoroethyl intermediate to the third transition state, we can also see that it is relatively easy to migrate a β -fluorine to the Zr center, further confirming the assertion that Zr interacts strongly with first row heteroatoms.

Comparison to the Calculated Hydrozirconation of CH_2CH_2 . It was found¹⁷ that ethylene insertion into the Zr-H bond of Cp_2ZrHCl occurred between the chloride and hydride ligands, as opposed to attacking from the side opposite to the Cl ligand. The difference in activation energy between these two transition states, 14.7 kcal/mol at the MP2 level of theory, was said to result from the smaller distortion of the complex required to access the transition state in the “inside” insertion case (Figure 8).

The mechanistic preference is similar to the one just discussed for the reaction of Cp_2ZrHCl with vinyl fluoride; in both cases, the faster insertion occurred from “inside.” Although the

calculation methods differ (and so energies cannot be compared exactly), this qualitative result confirms that a heteroatom on the olefin does not fundamentally alter the mechanism.

Minima for the β -F Ethyl Intermediates. Perhaps one of the most surprising results of this study was that β -fluoro agostic interactions give very little or no stabilization to the metal fragment (Figure 7). For example, **5** clearly has no interaction of the fluorine with the metal center. The Zr-F distance is quite long (4.538 Å) and there is no stretching of the C-F bond. **4** is the very weakly agostic β -fluoro intermediate seen in the “inside” reaction pathway. The two are basically conformers of each other, and differ only by 1.8 kcal/mol (well within the expected <3 kcal/mol difference for conformers). On the other hand, the -16.4 kcal/mol structure **3** (the β -F agostic intermediate from the “outside” pathway) is strongly agostic. In addition to a short Zr-F distance of 2.416, the C-F bond is clearly stretched (nearly 0.07 Å from the middle structure). However, the agostic structure is nearly 5 kcal/mol higher in energy than its nonagostic counterpart!

Since none of these structures show any agostic hydrogen interactions, the energies are not influenced by such factors. These structures, however, do illustrate that the inside LUMO is preferred. That is, when fluorine does interact with the zirconium center, it does so with overlap of the inside orbital. The lower energy of the “inside” insertion transition state also serves to confirm this.

However, the fact that the Zr/F interaction leads to a less stable conformation is counterintuitive. It not only contradicts the generalization that Zr prefers to interact with first row heteroatoms, it also goes against the intuitive response that a $16 e^-$ complex is a Lewis acid. There may be several reasons for this observed paradox. First, there is a marked increase in the Cl-Zr-C_α angle in **3** as compared to **5**, as well as a marked stretch in the Zr-C_α bond (2.403 vs 2.297 Å). This distortion from the optimized structure may cause a poor overlap between the carbon and zirconium orbitals. Second, the C-F bond is being stretched; this demands an energetic price, due to the strength of the C-F bond. For example, lengthening the CF bond in CFH_3 by 0.07 Å is calculated to cost 1.5 kcal/mol. Third, in contrast to **5**, which is staggered around the C-C bond, the fluoroethyl **3** is forced to be eclipsed. This, too, costs some energy in steric repulsion. F/Cl repulsion and a reduction in the Lewis acidity of Zr because of π -stabilization from Cl also serve to destabilize **3**.

Several other β -fluoroethyl intermediates, corresponding to rotation around the C-C, Zr-C, or ring puckering (from the strongly agostic species), were also found. In all cases, they were essentially isoenergetic (± 0.5 kcal/mol) with those structures reported here.

Interactions of α -Fluoro Species. We have also calculated structures resulting from the “wrong” insertion regiochemistry, species where fluorine is on C_α. When examining these minima, strong α -fluoro/Zr interactions were again seen to deliver negligible stabilization, as in the β -fluoro case (Figure 9). For example, **6** has little if any Zr-F interaction. Not only is the distance fairly long, the Zr-C_α-F bond angle is very close to tetrahedral, at 108.8°. This also serves to show that the best Zr acceptor orbital is *not* “outside.” Contrast this with **7**, which involves donation to the “inside” acceptor orbital of Zr. Not only is the Zr-F distance considerably shorter, but two other indicators of agostic interaction are present as well: namely, the C-F bond stretch and the marked decrease in the Zr-C_α-F angle (to 72.0°). It is obvious, then, that **7** has a much greater degree of interaction between the Zr and F. However, just as in

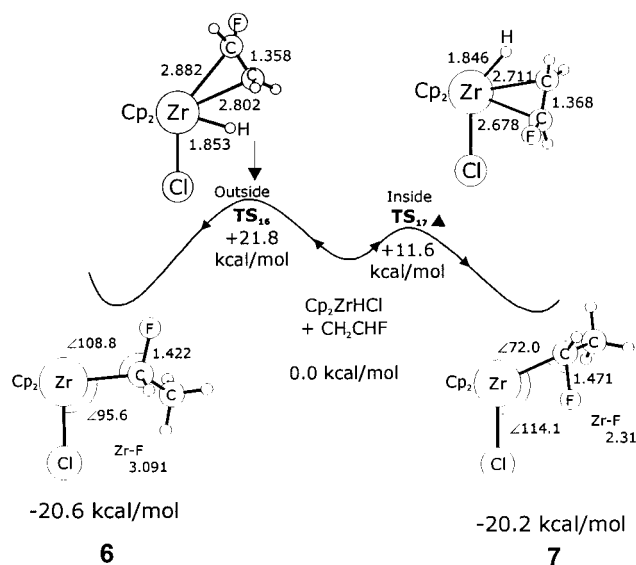


Figure 9. α -Fluoroethyl reaction pathways, with selected bond distances (Å), angles (deg), and relative energies in kcal/mol

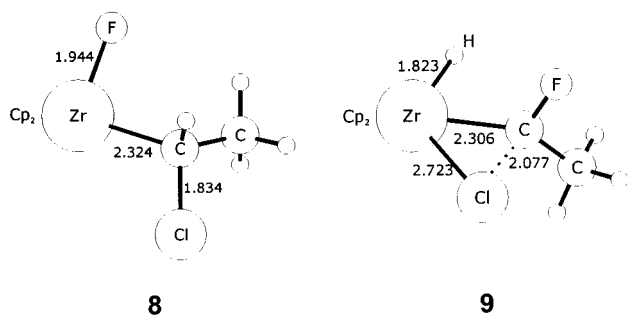


Figure 10. "Carbene" geometries.

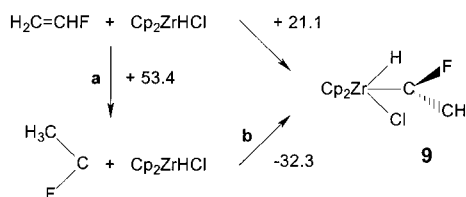
the β -F intermediates, there is no energetic stabilization derived from this interaction. Any stability from the Zr–F interaction is thus offset by the cost of increasing the C/Zr/Cl angle from 95.6° in **6** to 114.1° in **7**. One other conformer (rotation about the Zr–C $_{\alpha}$ bond to place F out of the plane) was also found. It, too, was essentially isoenergetic, having an energy of –20.1 kcal/mol.

Here, too, "outer" addition has a higher barrier than "inner" addition (Figure 9). Once again, the preference for the inside LUMO is seen. In both of these transition states, however, the energies are 2–4 kcal/mol higher than the corresponding energies for along the β -fluoro pathway that leads to the observed products. The degree of bond formation for this regiochemistry (taken from Zr–C $_{\alpha}$ distances) is slightly less in the "outside" insertion TS₁₆, and slightly more in the case of the "inside" TS₁₇ than for the other regiochemistry.

Stability of Carbenes Resulting from α -Fluoroethyl Isomerizations. One could imagine an isomerization process that would convert the α -fluoroethyl complexes into carbenes (either Cp₂ZrClF[CH(CH₃)] or Cp₂ZrClH[CF(CH₃)], shown in Figure 10). A potential energy surface search shows that the non- π -substituted carbene, Cp₂ZrClF[CH(CH₃)], is not a minimum. Instead, from various initial geometries, the carbene inserts into the Zr–Cl bond to form Cp₂ZrF[CHCl(CH₃)], **8**. Placing the carbene closer to the fluorine (making a smaller C $_{\alpha}$ /Zr/F angle) in the starting geometry for optimization still results in the insertion into the Zr–Cl bond.

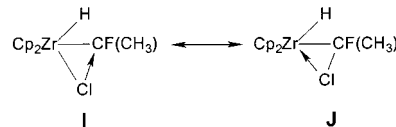
However, the π -substituted carbene, Cp₂ZrClH[CF(CH₃)], **9**, is a minimum (Figure 10). While high in energy compared to the separated Cp₂ZrHCl and CH₂CHF (+21.1 kcal/mol) because

Scheme 5



of lack of back-bonding, there is still a considerable thermodynamic gain in forming this carbene species from the separated carbene and zirconocene (Cp₂ZrHCl and C(F)(CH₃)) (Scheme 5). That is, the high energy of isomerizing vinyl fluoride to free CF(CH₃), **a**, 53.4 kcal/mol, costs more than the (considerable) binding energy of this carbene to Cp₂ZrHCl, **b**, 32.3 kcal/mol. The Zr/C distance, 2.306, is consistent with a single bond length.

9 also has some unexpected structural parameters. The Zr–Cl distance is much longer than in the starting Cp₂ZrHCl structure (2.723 vs 2.431 Å), and the Cl/Zr/C $_{\alpha}$ angle is exceptionally small (at 47.90°). This could perhaps be best explained by incipient donation of a Cl lone pair into the carbene p-orbital (**D**). It is apparently easier to contract the Cl/Zr/C $_{\alpha}$ angle than to pyramidalize the α -carbon (which remains essentially planar with the sum of angles around C $_{\alpha}$ in **9** equaling 358.0°) to promote better π -accepting. The chloride is still sufficiently far away (2.08 Å) such that no bond with C $_{\alpha}$ is actually made;



however, the sum of van der Waals radii for Cl and a benzene carbon is 3.55 Å.²¹ This further confirms that some interaction is taking place between the carbene carbon and the chloride, although the minimum energy structure is *not* at the "α-chloro agostic" alkyl stage (**J**), and certainly not the fully inserted species Cp₂ZrF(H)(CClF(CH₃)) analogous to the inserted product Cp₂ZrF(CHCl(CH₃)). This weak but non-negligible interaction between *cis* ligands is analogous to the "cis-effect" in *cis*-MH-(H₂) species.²² When we optimized geometry beginning from Cp₂Zr(H)(CClF(CH₃)) where C $_{\alpha}$ had an "ordinary" sp³ geometry, this again optimized to structure **9**, and thus the C–Cl bond is *nearly* cleaved.

Conclusions

This study provides confirmation of several factors that have been thought to be true concerning the reaction of Zr with olefins, but also reveals a number of surprises about the reaction of an early metal species with a hard fluoride functionality. As expected, the overall reaction is highly exothermic, forms a Zr–F bond, and fails to bind C₂H₄ to an unsaturated, but d⁰ product. Unlike the d⁶ example MHCIL₂ (M = Ru or Os), carbene products Cp₂ZrClF[CH(CH₃)] or Cp₂ZrClH[CF(CH₃)] are thermodynamically unfavorable due to lack of back-bonding from Zr(IV).

All of the surprises relate to the mechanism and the energies and structures of the fluoroethyl intermediates and transition states. The approach of either the slender F–C bond or the bulkier face (C/C π system) of vinyl fluoride is significantly easier in the "inside" orientation, as the "inside" unoccupied

(21) Bondi, A. J. *J. Chem. Phys.* **1964**, *68*, 441.

(22) Maseras, F.; Lledos, A.; Clot, E.; Eisenstein, O. *Chem. Rev.* **2000**, *100*, 601.

orbital is a better Lewis acid. The regiochemistry of addition of Zr–H across the CH₂=CHF bond is kinetically controlled by a **TS**₁₇ – **TS**₁₄ = 11.6 – 8.1 = 3.5 kcal/mol difference in activation energy, which calculates to a 0.3% predicted yield for the α -fluoroethyl product.

What is especially nonintuitive is the weakness of both α -F and β -F agostic interactions in the Cp₂ZrCl(fluoroethyl) intermediates, given the seemingly favorable hard acid/hard base interaction. “Intimate ion pairing” by C–F → Zr donation has become a major study area in catalyzed olefin polymerization.²³ We have resorted to steric repulsion and the energy cost of bending bond angles around Zr to rationalize these results, but the outcome remains fundamentally surprising.²⁴

Given that the σ -bond metathesis mechanism was initially devised for d⁰ cases where an oxidative addition/reductive elimination sequence is untenable, it is interesting that it is inferior here to β -H addition/ β -F elimination. Because there is here an energetically less costly mechanism, the σ -bond metathesis pathway fails to operate. The σ -bond metathesis transition state can be described as electrophile assisted (Zr(IV)) nucleophilic (H[–]) attack on the substituted vinyl carbon. It is noteworthy that these transition states show only modest disruption of the C=C double bonds, as judged by their length.

The absence of any η^2 -olefin intermediate, of either ethylene or vinyl fluoride, is noteworthy as well. While this claim might be viewed as subtle or even subjective, it can be made objective by the criterion of Zr/C bond length; there is no *intermediate* where anything approaching a typical Zr–C(olefin) bond distance is present. This does not create a significant kinetic barrier, however, since every TS *except the first* lies below the energy of the separated reactants; η^2 -C₂H₄ binding, if it occurred, would not accelerate product formation.

Experimental Section

General. All manipulations were performed using standard Schlenk line and glovebox techniques. Solvents were dried and distilled following standard protocols and stored in airtight solvent bulbs under argon. All reagents for which a synthesis is not given are commercially available from Aldrich or Lancaster and were used as received with no further purification. All NMR solvents were dried, vacuum-transferred, and stored in an argon-filled glovebox. ¹H, ¹⁹F, and ¹³C NMR were recorded on a Varian Gemini 2000, or Inova 700 spectrometer. Chemical shifts are reported in ppm and referenced to residual solvent peaks (¹H and ¹³C) or external CF₃COOH (neat), –78.5 ppm relative to CFCl₃ (¹⁹F).

Reaction of Cp₂ZrHCl with β -Methoxy Styrene. 10 mg (0.0392 mmol) of Cp₂ZrHCl was slurried in approximately 1 mL C₆D₆ and placed in an NMR tube. 5.5 μ L (0.0410 mmol, 1.05 equiv) of (C₆H₅)–CHCH(OCH₃) was added via syringe, and the tube shaken to thoroughly mix the reagents. Within 5 min, a noticeable yellow tint of the supernatant was apparent; after 2 h, the yellow solution was entirely homogeneous. Cp₂Zr(OMe)Cl, Cp₂(Cl)ZrCH₂CH₂Ph, and Cp₂(Cl)–ZrCHPhCH₃ were observed by NMR. ¹H NMR, COSY, HMQC, and DEPT experiments were used to confirm the observed products; Cp₂(Cl)ZrCH₂CH₂Ph, and Cp₂(Cl)ZrCHPhCH₃ were synthesized independently by the reaction of PhCHCH₂ with Cp₂ZrHCl and compared with literature results.²⁵ ¹H NMR (300 MHz, C₆D₆): Cp₂Zr(OMe)Cl, δ 5.73 (s, 10 H, Cp₂ZrClOMe), 3.64 (s, 3H, Cp₂ZrClOMe); Cp₂(Cl)Zr–CH₂CH₂Ph (major product), δ 7.22 (m, 5H, Cp₂(Cl)ZrCH₂CH₂Ph), 5.90 (s, 10H, Cp₂ZrCH₂CH₂Ph), 2.86 (m, 2H, Cp₂(Cl)ZrCH₂CH₂Ph), 1.31

(m, 2H, Cp₂(Cl)ZrCH₂CH₂Ph)—all CH₂ protons exhibited AA'XX' coupling; Cp₂(Cl)ZrCHPhCH₃ (minor product), δ 7.10 (m, 5H, Cp₂(Cl)ZrCHPhCH₃), 6.01 (s, 10H, Cp₂(Cl)ZrCHPhCH₃), 2.94 (q, 1H, Cp₂(Cl)ZrCHPhCH₃), 1.50 (d, J = 10 Hz, 3H, Cp₂(Cl)ZrCHPhCH₃).

Reaction of Cp₂ZrHCl with CH₂CHF. Cp₂ZrHCl (10.1 mg, 0.039 mmol) was slurried in approximately 0.5 mL of C₆D₆ and placed in an NMR tube under argon. CH₂CHF (1.502 equiv) was added via standard gas line techniques. The previously clear supernatant turned a pale yellow color and the reaction was nearly homogeneous after 1.5 h of agitation. ¹H NMR (400 MHz, C₆D₆): ethylene (δ 5.24(s)), Cp₂Zr–(CH₂CH₃)Cl²⁶ δ 1.08 (q, J = 7 Hz, 2H, Cp₂Zr(CH₂CH₃)Cl), 1.44 (t, J = 7 Hz, 3H, Cp₂Zr(CH₂CH₃)Cl), 5.75 (s, 10H, Cp₂Zr(CH₂CH₃)Cl). Due to the insolubility of dihalide species, only excess vinyl fluoride could be identified reliably in the ¹⁹F NMR spectra. Halide exchange products were also obtained. Unreacted CH₂CHF could be observed by NMR even when reacted as 0.90 equivalents. With identical conditions as above, Cp₂ZrHCl and CH₂CHF were reacted in *d*₈-THF, to better observe growth of dihalide products. Within 1 h, the solution was homogeneous and slightly yellow in color. (¹H NMR, 400 MHz): Cp₂ZrCH₂CH₃(Cl), δ 6.318 (s, 10H, Cp₂ZrClCH₂CH₃), 1.314 (t, J = 7.6 Hz, 3H, Cp₂ZrClCH₂CH₃), 0.970 (q, J = 7.6 Hz, 2H, Cp₂ZrClCH₂–CH₃); CH₂CH₂, δ 5.360 (s); other Cp resonances at δ 6.490, 6.437, 6.367 (assigned to Cp₂ZrF₂ by comparison to an authentic sample), 6.229. (¹⁹F, 376.5 MHz): δ 28.378, 2.051, –94.948, broad resonance at –140.

Reaction of Cp₂ZrHCl with 1,1 CH₂CF₂. Cp₂ZrHCl (10.0 mg, 0.039 mmol) was slurried in approximately 0.5 mL of C₆D₆ and placed in an NMR tube under argon. CH₂CF₂ (1.57 equiv) was added via standard gas line techniques. The slightly yellow solution appeared mostly homogeneous within 1.5 h. Excess CH₂CF₂, CH₂CHF, Cp₂Zr–(CH₂CH₃)Cl, and CH₂CH₂ were then visible in the ¹H and ¹⁹F NMR spectra.

Reaction of Cp₂ZrHCl with C₆H₅F. Cp₂ZrHCl (10.0 mg, 0.039 mmol) was slurried in approximately 0.5 mL of C₆D₆ and placed in an NMR tube under argon. C₆H₅F (4.0 μ L, 0.0426 mmol, 1.1 equiv) was added via syringe. No change was observed by NMR after 3 days tumbling at room temperature. The mixture was still heterogeneous with a clear supernatant. Heating of the NMR tube at 60° for approximately 1 h produced a homogeneous purple solution, from the decomposition of Cp₂ZrHCl.²⁷ The ¹H and ¹⁹F NMR of the C₆H₅F was unchanged, and no C₆H₆ was produced. Identical results were obtained when a large excess of C₆H₅F (1:1 C₆H₅F/C₆D₅CD₃ as solvent) or a catalytic amount (0.1 equiv) of C₆H₅F was used. No reaction occurred as well when C₆H₆ or *d*₁₂-cyclohexane were used as solvents.

Similar methods employed with 1,3 C₆H₄F₂, 1,4 C₆H₄F₂, 4-fluoroanisole, and C₆F₆ also showed no reaction with Cp₂ZrHCl even with extended reaction time. Heating caused the decomposition of Cp₂ZrHCl.

Synthesis of Cp₂ZrF₂. This procedure is a slight modification of Seyam's preparation.²⁸ Cp₂ZrCl₂ (1.6 g, 5.47 mmol) was dissolved in 150 mL of acetone (dried with MgSO₄ and molecular sieves and degassed prior to use). AgBF₄ (2.189 g, 11.25 mmol, 2.06 equiv) dissolved in 50 mL of acetone was added dropwise through an addition funnel wrapped in aluminum foil over 30 min at 0 °C. A white solid (AgCl) formed on contact. The reaction solution was stirred for an additional 15 min at room temperature. The yellow supernatant was removed via cannula and filtered. The volume was then reduced to approximately 30 mL, and 60 mL of dry ether was layered on top. Recrystallization at –40° afforded a very pale beige solid. Isolated yield, 68%. ¹H NMR (*d*₈-THF, 400 MHz): 6.38 (s, Cp₂ZrF₂). ¹⁹F NMR (*d*₈-THF, 376.5 MHz): –157.3 (br s).

Computational Details

All calculations were performed with the Gaussian 98 package²⁹ at the B3PW91³⁰ level of theory. Basis sets used include LANL2DZ for Zr and Cl, 6-31G for all Cp carbons and hydrogens,³¹ 6-31G* for fluorine and the fluoroethylene carbons, and 6-31G** for the hydride

(23) Chen, E. Y.; Marks, T. J. *Chem. Rev.* **2000**, *100*, 1391.

(24) A referee disagrees that this is surprising and feels it is caused by transfer to Zr of “...considerable π charge from the Cp ligands...”

(25) (a) Nelson, J. E.; Bercaw, J. E.; Labinger, J. A. *Organometallics* **1989**, *8*, 2484. (b) Erker, G.; Kropp, K.; Atwood, J. L.; Hunter, W. E. *Organometallics* **1983**, *2*, 1555–1561. (c) Chirik, P. J.; Day, M. W.; Labinger, J. A.; Bercaw, J. E. *J. Am. Chem. Soc.* **1999**, *121*, 10308.

(26) Gell, K. I.; Posin, B.; Schwartz, J.; Williams, G. *J. Am. Chem. Soc.* **1982**, *104*, 1846.

(27) Wailes, P. C.; Weigold, H. *J. Organomet. Chem.* **1970**, *24*, 405.

(28) Seyam, A.; Samha, H.; Hodali, H. *Gazz. Chim. Ital.* **1990**, *120*, 527.

and fluoroethylene hydrogens. The basis set LANL2DZ is the Los Alamos National Laboratory ECP plus a double- ζ valence on Zr and Cl.³² Because of the electronegativity of fluorine, and thus the probable

(29) Frisch, M. J.; Trucks, G. W.; Schlegel, H. B.; Scuseria, G. E.; Robb, M. A.; Cheeseman, J. R.; Zakrzewski, V. G.; Montgomery, J. A., Jr.; Stratmann, R. E.; Burant, J. C.; Dapprich, S.; Millam, J. M.; Daniels, A. D.; Kudin, K. N.; Strain, M. C.; Farkas, O.; Tomasi, J.; Barone, V.; Cossi, M.; Cammi, R.; Mennucci, B.; Pomelli, C.; Adamo, C.; Clifford, S.; Ochterski, J.; Petersson, G. A.; Ayala, P. Y.; Cui, Q.; Morokuma, K.; Malick, D. K.; Rabuck, A. D.; Raghavachari, K.; Foresman, J. B.; Cioslowski, J.; Ortiz, J. V.; Stefanov, B. B.; Liu, G.; Liashenko, A.; Piskorz, P.; Komaromi, I.; Gomperts, R.; Martin, R. L.; Fox, D. J.; Keith, T.; Al-Laham, M. A.; Peng, C. Y.; Nanayakkara, A.; Gonzalez, C.; Challacombe, M.; Gill, P. M. W.; Johnson, B. G.; Chen, W.; Wong, M. W.; Andres, J. L.; Head-Gordon, M.; Replogle, E. S.; Pople, J. A. *Gaussian 98*, revision A.7; Gaussian, Inc.: Pittsburgh, PA, 1998.

(30) Becke, A. D. *Phys. Rev.* **1988**, *A38*, 3098.; Becke, A. D. *J. Chem. Phys.* **1993**, *98*, 1372; Becke, A. D. *J. Chem. Phys.* **1993**, *98*, 5648; Perdew, J. P.; Wang, Y. *Phys. Rev. B* **1991**, *45*, 13244.

(31) Hariharan, P. C.; Pople, J. A. *Theor. Chim. Acta* **1973**, *28*, 213.

(32) Hay, P. J.; Wadt, W. R., *J. Chem. Phys.* **1985**, *82*, 270; Wadt, W. R.; Hay, P. J. *J. Chem. Phys.* **1985**, *82*, 284; Hay, P. J.; Wadt, W. R. *J. Chem. Phys.* **1985**, *82*, 299.

inclusion of some d-orbital character in its bonding orbitals, in all DFT calculations discussed here polarization functions were included on all non-Cp ligands. All calculations were performed with C_1 symmetry, and all stationary points were characterized as minima or transition states by a frequency analysis, which was also used to compute zero-point energy corrections without scaling. For the 4-centered, σ -bond metathesis transition states, a grid method was employed to find the TS. The C–H distance was frozen to values between 2.6 and 1.4, and additional dihedrals corresponding to $\angle F-H-Zr-Cl$ and $\angle C_{\alpha}-H-Zr-Cl$ were frozen to 0°. The structures were allowed to optimize, and a transition-state calculation was started from the highest-energy structure that had not dissociated. Further optimization of the obtained structure (with three imaginary frequencies) resulted in a true transition state. All transition states were confirmed to lie on the reaction pathway by distorting the complex along the imaginary frequency and optimizing the resulting structure.

Acknowledgment. This work was supported by the donors of the Petroleum Research Fund. L.A.W. gratefully acknowledges the National Science Foundation for a graduate fellowship.

JA0024340